Bojan ŠTUMBERGER[1,2], Dalibor IGREC[1,3], Amor CHOWDHURY[1,3], Miralem HADŽISELIMOVIC[1,2]

University of Maribor, Faculty of Energy Technology (1)
University of Maribor, Faculty of Electrical Engineering and Computer Science (2), Margento R&D d.o.o. (3)

Design of synchronous reluctance generator with dual stator windings and anisotropic rotor with flux barriers

***Abstract**. Appropriate design of synchronous reluctance machine with dual stator winding and anisotropic rotor with flux barriers in generator operation mode is investigated. Finite element analysis is employed in order to determine the machine performance. Two different designs for synchronous reluctance generator with dual stator windings and the same anisotropic rotor with flux barrier are presented.*

***Streszczenie.** W artykule przedyskutowano właściwe projektowanie maszyny reluktancyjnej z podwójnym uzwojeniem stojana oraz anizotopowym wirnikiem z przegrodami strumieniowymi, pracującej w trybie generatorowym. W celu wyznaczenia działania maszyny użyta została metoda elementów skończonych. Przedstawione zostały dwa projekty synchronicznego, reluktancyjnego generatora z podwójnym uzwojeniem stojana oraz anizotropowym wirnikiem z przegrodami strumieniowymi. (**Projekt synchronicznego reluktancyjnego generatora z podwójnym uzwojeniem stojana i wirnikiem anizotropowym z przegrodami strumieniowymi**).*

Keywords: synchronous machine, reluctance generator, dual stator windings.
Słowa kluczowe: maszyna synchroniczna, generator reluktancyjny, podwójne uzwojenia stojana.

Introduction

In wind-power generation different variable-speed generator types can be found. Rotors of electric generators are usually mechanically coupled to the wind turbines through a gearbox in order to maintain small machine diameter, while the use of large-diameter low-speed direct-drive generators is less frequent.

The use of doubly-fed wound-rotor induction generators (DFIGs) in wind-power generation is dominant, although dual-winding induction generators (DWIGs) with special nested-loop rotors can be found as well [1-4].

The main drawback of the most frequently used DFIGs is the presence of slip rings which can be problematic from the aspect of reliability and generator maintenance costs. Due to the absence of the slip rings the brushless doubly-fed reluctance machine (BDFRM) can be a realistic alternative to the DFIG. Similarly to the DFIG, the BDFRM has a primary winding (normally called power winding or main winding) and a secondary winding (normally called excitation winding or control winding). Contrary to the DFIG the excitation winding of BDFRM is placed in the stator. Because of this special feature the BDFRG can be called dual stator winding reluctance generator (DSWRG) as well.

Usually the main and the excitation winding of DSWRG have different number of poles and are manufactured in distributed winding technology [5-12]. The rotor of the DSWRG has to provide efficient magnetic coupling between the excitation and the main winding. The most efficient rotor structure of DSWRG is similar to the rotor structure of an ordinary multiple-barrier synchronous reluctance machine [5-12], [13-15]. For the successful magnetic coupling and good machine performance the correct correlation between the number of rotor pole pairs p_r , the number of pole pairs of the excitation winding p_s and the number of pole pairs of the main winding p_p have to be taken into account: $p_r=0.5(p_s+p_p)$. In the steady-state conditions the frequency of the induced voltage in the main winding f_p (Hz) is connected with the rotor rotational speed n_r (rev/min) and frequency of the excitation current in the excitation winding f_s by: $f_p=(2n_rp_r/60)-f_s$.

Due to the many different possible combinations of pole pair number of main and excitation winding in connection with the number of stator slots and the number of flux barriers per rotor pole, different structures of DSWRG have to be investigated by using finite element method in order to determine the best possible DSWRG construction.

Basic DSWRG design for the four-pole radially-laminated rotor construction (rotor design with three rotor flux barriers per pole is used) and stator with 36 stator slots will be presented in this work. Two-pole three-phase single layer winding is used for the excitation winding and six-pole three-phase single layer winding is used for the main winding in stator design with the 36 stator slots. In this case the two-pole and the six-pole windings share the same stator slots.

An alternative to the above mentioned design of DSWRG where the main and the excitation winding have different number of poles can represent the DSWRG design where the main and the excitation winding have the same number of poles as is the rotor pole number. In this case the main winding system and the excitation winding system represent two three-phase systems whose magnetic axes are shifted between each other for thirty electrical degrees. The main and the excitation three-phase system are in this case without any mutual electrical connection. Alternative design of DSWRG can represent stator with 24 stator slots and four-pole single layer main and excitation winding system in connection with the same four-pole radially laminated rotor construction as it is used for the basic DSWRG rotor design.

The basic DSWRG design with different number of poles for the main and for the excitation winding system has already been presented in a different publication [5-12], while the DSWRG design with the same number of poles for the main and for the excitation windings has not been yet presented in the literature.

Method of analysis

To obtain the field distributions and the loci of local flux density vectors in the machine, a series of magneto-static field calculations for a complete cycle of field variation was computed by 2D FEM, using the basic equation:

$$\mathrm{rot}(\nu\,\mathrm{rot}(\boldsymbol{A})) = \boldsymbol{J}_0 + \mathrm{rot}\boldsymbol{M} \tag{1}$$

where ν denotes the reluctivity, $\boldsymbol{A}$ is the magnetic vector potential, $\boldsymbol{J}_0$ is the current density and $\boldsymbol{M}$ is the magnetization of the permanent magnets.

The non-linearity of the used iron core material was accounted for with a single-valued *B-H* curve., The magnetic conditions over a complete cycle of magnetic field variation were calculated in discrete equidistant time steps by shifting the rotor position and simultaneously changing the stator excitation. For terminal voltage, input power, output power and efficiency calculation, an already proven procedure has been used [13].

DSWRG description and presentation of results

In order to reveal appropriate design of the DSWRG, two different concepts with the same rotor structure have been taken into consideration. The first concept is based on the different number of poles for the main and the excitation winding (design DSWRG (A)) and the second one is based on the same number of poles for the main and the excitation winding (design DSWRG (B)). For the base size of the DSWRG machine, the IEC 71 frame size has been selected. For rotor design the geometry used for the permanent magnet assisted reluctance rotor was used [13]. The picture of rotor lamela is presented in Fig. 1, while the unusual winding arrangement for the DSWRG (B) design is presented in Fig. 2. Two different DWSRG design concepts were compared for the same speed level in a situation where the total numbers of ampere-turns are comparable. Calculation results are presented in Figs. 3-14.

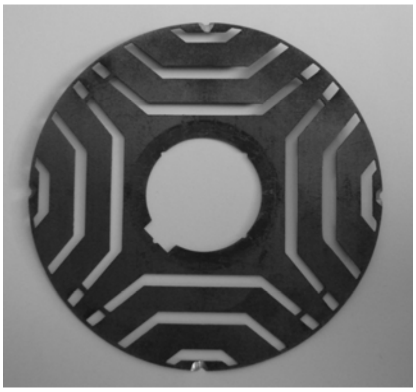

Fig. 1. Picture of rotor lamella, four poles, three flux-barriers per pole.

From the results of flux density distribution presented in Figs. 5-6 it is clear that DSWRG (A) design exhibits higher saturation in stator yoke than DSWRG (B) design. However, this is not true anymore in the case when the main winding is loaded by the electrical load, which can be seen for Figs. 7-8. DSWRG (A) design exhibits imperfect non-symmetrical induced voltages, while DSWRG (B) design exhibits perfect symmetrical induced voltages (results presented in Fig. 9 and Fig. 11). The same situation regarding the symmetry of phase voltages can be observed in the case when the main winding of DSWRG machine is loaded by electric load as well. At the same number of ampere-turns in the excitation and the main winding, the DSWRG (B) design exhibits higher phase voltages than DSWRG (A) design. Both DSWRG designs can supply electric loads with near unity power factor, which can be seen in Fig. 10 and Fig. 13.

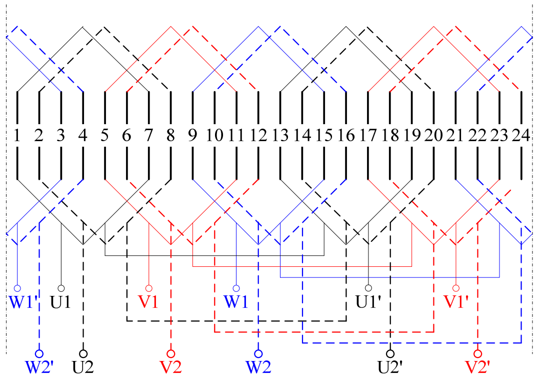

Fig. 2. Winding arrangement for the DSWRG with the same number of poles for the excitation (solid line) and for the main winding (dashed line), DSWRG (B).

Conclusion

From the presented results it can be concluded that DSWRG (B) design can be a serious alternative to the known DSWRG designs. With the proper excitation control both DSWRG designs can work with near unity power factor. The main drawback of the DSWRG (B) design presents the fact that the frequency of the main winding voltage is directly dependent on the rotor speed, when small torque ripple has to be assured.

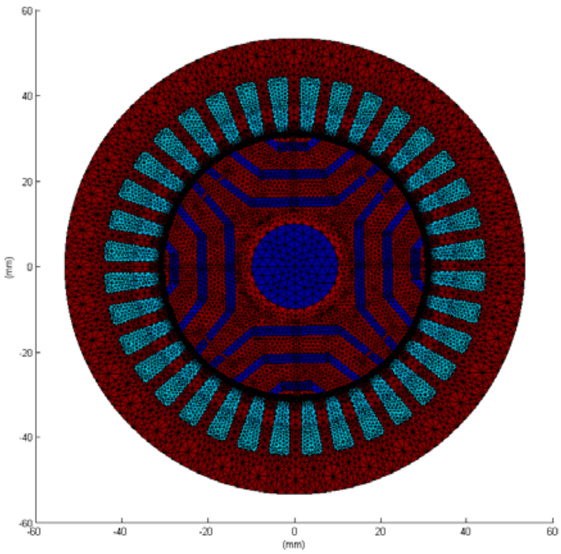

Fig. 3. DSWRG discretization, DSWRG (A)-36 stator slots .

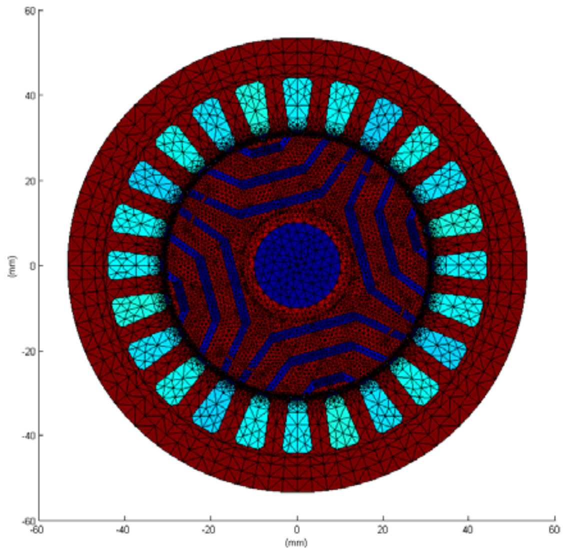

Fig. 4. DSWRG discretization, DSWRG (B)-24 stator slots .

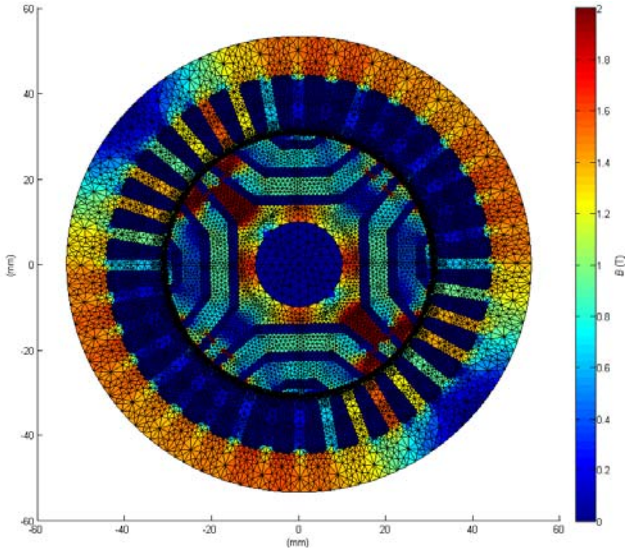

Fig. 5. Flux density distribution for DSWRG (A), only excitation winding is active, RMS value of phase current is 1 A.

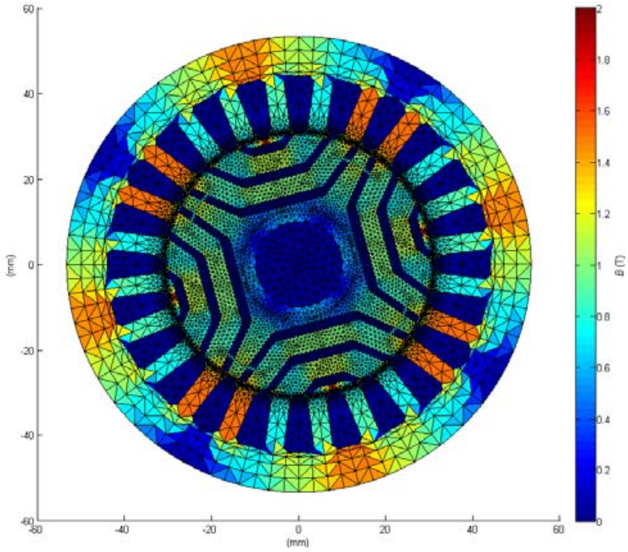

Fig. 6. Flux density distribution for DSWRG (B), only excitation winding is active, RMS value of phase current is 1.7 A..

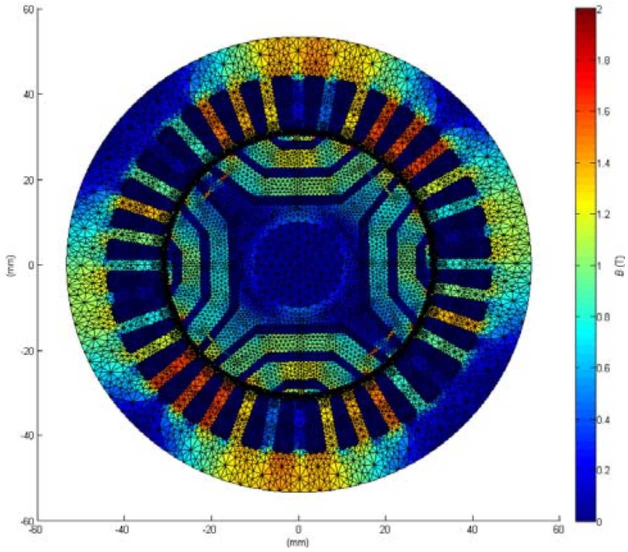

Fig. 7. Flux density distribution for DSWRG (A), the excitation winding and the main winding are active, RMS value of phase current in the main and the excitation winding is 1 A.

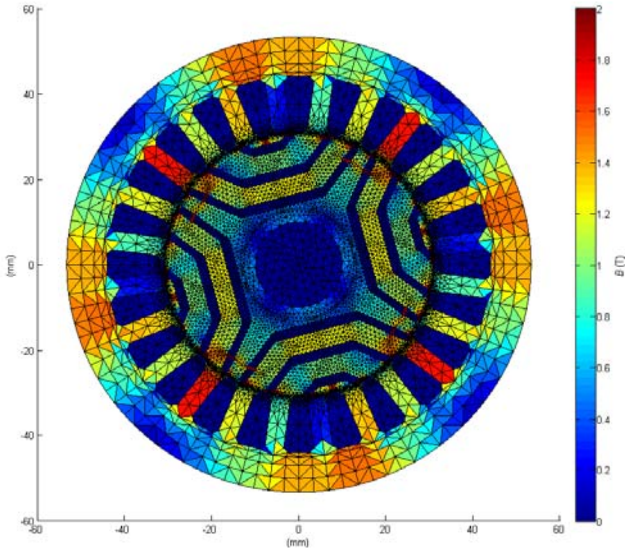

Fig. 8. Flux density distribution for DSWRG (B), the excitation winding and the main winding are active, RMS value of phase current in the main and the excitation winding is 1.7 A.

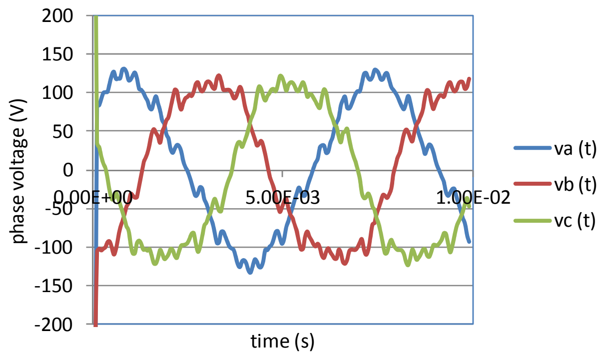

Fig. 9. Induced voltage waveform in the main winding of DSWRG (A) at 3000 rpm, RMS value of the phase current in the excitation winding is 1 A, frequency of the excitation current is 50 Hz, frequency of the main winding voltage is 150 Hz.

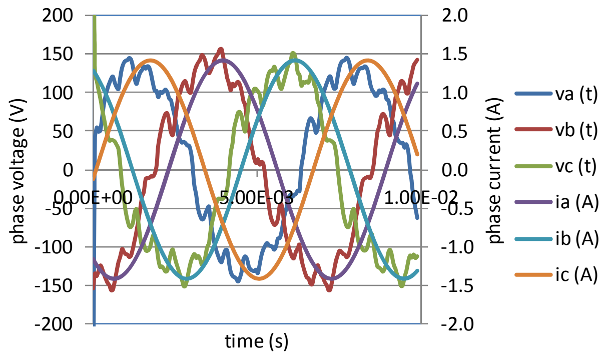

Fig. 10. Phase voltage and current waveforms in the main winding of DSWRG (A) at 3000 rpm under load, RMS value of the phase current in the excitation winding and the main winding is 1 A, frequency of the excitation current is 50 Hz, frequency of the main winding voltage is 150 Hz.

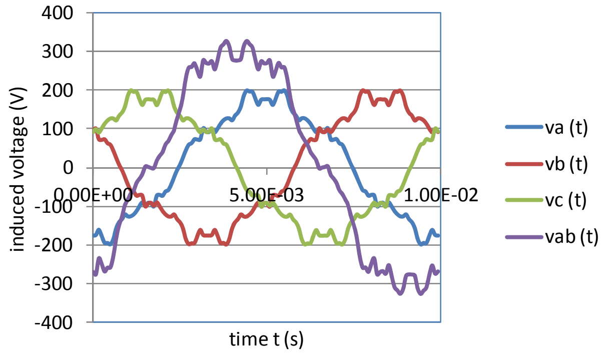

Fig. 11. Induced voltage waveform in the main winding of DSWRG (B) at 3000 rpm, RMS value of the phase current in the excitation winding is 1.7 A.

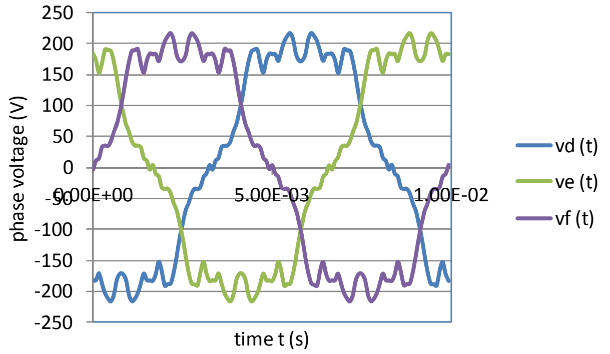

Fig. 12. . Voltage waveform in the excitation winding of DSWRG (B) at 3000 rpm, RMS value of the phase current in the excitation winding is 1.7 A.

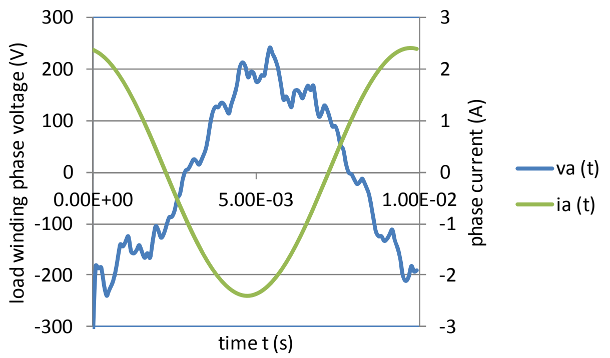

Fig. 13. Phase voltage and current waveforms in the main winding of DSWRG (B) at 3000 rpm under load, RMS value of the phase current in the excitation winding and the main winding is 1.7 A.

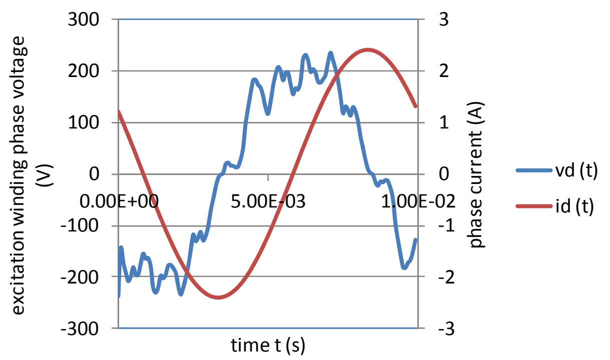

Fig. 14. Phase voltage and current waveforms in the excitation winding of DSWRG (B) at 3000 rpm under load, RMS value of the phase current in the excitation winding and the main winding is 1.7 A.

REFERENCES

[1] E. Spooner, A.C. Williamson, »Mixed Pole Windings And Some Applications«, *IEE Proceedings*, Vol. 137, No. 2, pp. 89-97, March, 1990

[2] S. Williamson, A. C. Ferreira, A. K. Wallace, »Generalised Theory Of The Brushless Doubly-Fed Machine. Part I : Analysis«, *IEE Proceedings-Electric Power Applications*, Vol. 144, No. 2, pp. 111-122, March, 1997

[3] S. Williamson, A. C. Ferreira, »Generalised Theory Of The Brushless Doubly-Fed Machine. Part 2: Model Verification And Performance«, *IEE Proceedings-Electric Power Applications*, Vol. 144, No. 2, pp. 123-129, March, 1997

[4] F. Barati, S. Shao, E. Abdi, H. Oraee, R. McMahon, »Generalized Vector Model for the Brushless Doubly-Fed Machine With a Nested-Loop Rotor«, *IEEE Transactions On Industrial Electronics*, Vol. 58, No. 6, June, 2011

[5] T. Fukami, M. Momiyama, K, Shima, »Steady-State Analysis of a Dual-Winding Reluctance Generator With a Multiple-Barrier Rotor«, *IEEE Transactions on Energy Conversion*, Vol. 23, No. 2, pp. 492-498, June, 2008

[6] R. E. Betz, M. G. Jovanović, »The Brushless Doubly Fed Reluctance Machine and the Synchronous Reluctance Machine - A Comparison«, *IEEE Transactions on Industry Applications*, Vol. 36, No. 4, pp. 1103-1110, July/August, 2000

[7] F. Valenciaga, P. F. Puleston, »Variable Structure Control of a Wind Energy Conversion System Based on a Brushless Doubly Fed Reluctance Generator«, *IEEE Transactions on Energy Conversion*, Vol. 22, No. 2, pp. 499-506, June, 2007

[8] D. G. Dorrell, M. Jovanović, »On the Possibilities of Using a Brushless Doubly-Fed Reluctance Generator in a 2 MW Wind Turbine«, *Industry Applications Society Annual Meeting, 2008. IAS '08. IEEE*, pp. 1-8, October, 2008

[9] Q. Zhang, H. Liu, »Comparative Study of Brushless Doubly Fed Machine with Different Rotor Structures Used in Wind Power Generation System«, *Power and Energy Engineering Conference (APPEEC), 2010 Asia-Pacific*, pp. 1-4, March, 2010

[10] D. G. Dorrell, A. M. Knight, R. E. Betz, »Issues with the Design of Brushless Doubly-Fed Reluctance Machines: Unbalanced Magnetic Pull, Skew and Iron Losses«, *Electric Machines & Drives Conference (IEMDC), 2011 IEEE International*, pp. 663-668, May, 2011

[11] D. G. Dorrell, A. M. Knight, R. E. Betz, »Improvements in Brushless Doubly Fed Reluctance Generators Using High-Flux-Density Steels and Selection of the Correct Pole Numbers«, *IEEE Transactions on Magnetics*, Vol. 47, No. 10, pp. 4092-4095, October, 2011

[12] A. M. Knight, R. E. Betz, D. Dorrell, »Design And Analysis Of Brushless Doubly Fed Reluctance Machines«, *Energy Conversion Congress and Exposition (ECCE), 2011 IEEE*, pp. 3128-3135, September, 2011

[13] B. Štumberger, G. Štumberger, M. Hadžiselimović, T. Marčič, P. Virtič, M. Trlep, V. Goričan, »Design and finite-element analysis of interior permanent magnet synchronous motor with flux barriers«, *IEEE trans. magn.*, Vol. 44, No. 11, pp. 4389-4392, November, 2008

[14] B. Štumberger, V. Goričan, G. Štumberger, M. Hadžiselimović, T. Marčič, M. Trlep, »Performance evaluation of synchronous reluctance motor in BLDC drive«, *Prz. Elektrotech.*, pp. 147-149, 2009

[15] B. Štumberger, R. Pulko, V. Goričan, M. Hadžiselimović, »Influence of permanent magnet material on characteristics of permanent magnet assisted reluctance motor«, *Prz. Elektrotech.*, Vol. 85, Iss. 12, 2010

Authors: *Bojan Štumberger, Miralem Hadžiselimović, University of Maribor, Faculty of Energy Technology, Hočevarjev trg 1, 8270 Krško, Slovenia, Dalibor Igrec, Amor Chowdhury, Margento R&D d.o.o., Gosposvetska cesta 84, 2000 Maribor, Slovenia*
E-mail: bojan.stumberger@uni-mb.si.